Front. Earth Sci. 2020, 14(1): 63–76
https://doi.org/10.1007/s11707-019-0805-5

RESEARCH ARTICLE

Coupled model constructed to simulate the landslide dam flood discharge: a case study of Baige landslide dam, Jinsha River

Hongjie WANG[1,2,3], Yi ZHOU (✉)[1,3], Shixin WANG[1,3], Futao WANG (✉)[1,3]

1 Aerospace Information Research Institute, Chinese Academy of Sciences, Beijing 100101, China
2 University of Chinese Academy of Sciences, Beijing 100101, China
3 Institute of Remote Sensing and Digital Earth, Chinese Academy of Sciences, Beijing 100101, China

Abstract Landslide dam, always triggered by the strong earthquake and heavy rain, is a common natural disaster around the world. In this study, a coupled model was built by combining DB-IWHR model and the two-dimensional hydrodynamic model to simulate the landslide dam flood discharge. We mapped the maximum Baige landslide dam flood inundated area based on Gaofen-1 imagery, and then simulated the process of Baige landslide dam flood discharge using this coupled model. It was proved that, with 80.05% F values, the coupled model was suitable to simulate the process of landslide dam flood discharge. Lastly, multiple scenarios were simulated respectively by setting varying width and depth of spillway. The results of scenarios 1–4 indicated that spillway width presented low sensibility to the peak flow in spillway and the time of its arrival, and similarly to the water depth at river cross-section and the inundated area. Water depth at river cross-section and the inundated area decreased as spillway width increased. Even if spillway width varied at 10 m interval, the average variation of water depth was less than 1.82 m and the variation of inundated area was less than 2.85%. However, the results of scenarios 5–8 indicated that spillway depth was sensitive to the peak flow in spillway and its arrival time, and also to water depth at river cross-section and the inundated area. Water depth at river cross-section and the inundated area increased first and then started to drop with spillway depth kept decreasing. When spillway depth varied at only 2 m interval, the average variation of water depth at river cross-section basically exceeded 2 m and the variation of inundated area was more than 2.85%.

Received June 21, 2019; accepted November 5, 2019

E-mails: zhouyi@radi.ac.cn (Yi ZHOU); wangft@aircas.ac.cn (Futao WANG)

Keywords landslide dam, scenario simulation, flood discharge

1 Introduction

Landslide dams are common disasters that occur frequently in tectonic active mountain zone with the narrow and abrupt valleys, and always form landslide lake with potentially harmful on account of river-blocking obstructions (Costa and Schuster, 1988). Strong earthquake and heavy rainfall are the main factors triggering landslide dams (Keefer, 1984; Schuster, 1995; Chen et al., 2006; Evans et al., 2011; Wang et al., 2013). For example, more than 800 landslide dams were triggered by the M_w 7.9 Wenchuan earthquake in Sichuan Province in China (Gorum et al., 2011; Fan et al., 2012). Once the landslide dam formed, personal safety and property would be threatened by floods triggered by landslide lake level rising and mass and the rapid release of water (Cenderelli, 2000; Dai et al., 2005; O'Connor and Beebee, 2009). Several studies have concentrated on the following aspects: 1) research on landslide-dam inventories (Costa and Schuster, 1991; Chai et al., 1995; Korup, 2004; Hermanns et al., 2011; Fan et al., 2012); 2) research on single case study, containing forecasting the form of landslide dams (Mandrone et al., 2007; Chen et al., 2015a), the assessment of landslide dam stability by the dam parameters and empirical formula (Ermini and Casagli, 2003; Korup and Tweed, 2007; Dong et al., 2009; Xu et al., 2009; Wang et al., 2018a); 3) forecasting calculating peak discharge of dam break (Evans, 1986; Walder and O'Connor, 1997; Cook, 2008) and the assessment of dam break flood hazard (Peng and Zhang, 2012; Basabe, 2013).

However, as a natural disaster, landslide dam usually forms the landslide lake by blocking the river, and causing significant hazards around the world in case of landslide dam break (Korup, 2002; Dai et al., 2005). For example, the Dadu river landslide dam, triggered by the strong earthquake in Sichuan Province of China in 1786, failed ten days later, and the suddenly catastrophic flood caused over 100000 deaths in the downstream (Dai et al., 2005). Hence, how to mitigate landslide dam disaster is very important. However, the method of landslide dam disaster mitigation and relief was flood discharge using spillway-through manual excavation or exploding nowadays (Xu et al., 2009). In addition, spillway width and depth were increasing in the process of landslide dam flood discharge, and landslide dam flood flow was highly unsteady flow along the riverbed and inundated both sides of flood plain. However, there was not any clear and professional model to simulate the progress of landslide dam flood discharge for disaster mitigation and relief. For instance, the Baige landslide dam flood discharge has caused the biggest flood in Lijiang in recent years. Hence, how to build the model for guiding landslide dam flood discharge is very important to relieve landslide dam disaster.

Landslide dam, as a natural dam, is similar to artificial dam. Meanwhile, we also consider artificial spillway as a special dam breach, which will be a new viewpoint for landslide dam flood discharge model constructed. Now the research on dam break flood discharge was reflected in the following two aspects: on the one hand, concentrating on the development of dam breach, we usually adopted model experiment analysis (Morris and Galland, 1988; Zhang et al., 2009), empirical formula method (Singh et al., 1988; Xu and Zhang, 2009), and numerical simulation method (Fread, 1984; Fread, 1988; Wu, 2013). In recent 50 years, a large number of dam-break models have been built. Especially Chen et al. (2015b) proposed DB-IWHR model based on previous study (Cristofano, 1965; Brown and Rogers, 1981; Fread, 1984; Costa, 1985; Fread, 1988; Singh et al., 1988; Walder and O'Connor, 1997; Wang and Bowles, 2006; Chang and Zhang, 2010; Wu, 2013). The advantages of DB-IWHR model including transparent calculation progress and the improved correctness of calculation results, as well as being less sensitive to input parameters for dam break analysis, which has been already verified by landslide dam-break measured data (Wang et al., 2016).

On the other hand, it focused on the study of flood inundation model. In this field, many scholars tried to figure out the processes of flood flow and evaluate the risk of flood taking advantage of Geographic Information System (GIS) (Ahmad and Verma, 2018). Three categories including the empirical methods (Smith, 1997; O'Connor and Costa, 2004), the hydrodynamic models (Roberts et al., 2015; Brunner, 2016) and the simplified methods (Pender, 2006) were summarized (Teng et al., 2017). Hydrodynamic models have been widely used to achieve flood mapping (Knebl et al., 2005; Gallegos et al., 2009; Renschler and Wang, 2017; Li et al., 2019; Yin et al., 2019) and simulated flood scenario in combination with empirical methods and simplified methods. One-dimensional hydrodynamic model provided no flow field information and had complex operation (Viero et al., 2014). In this study, we adopted the two-dimensional hydrodynamic model to simulate landslide dam flood discharge.

Although scholars have obtained lots of achievements on dam-break model and flood inundation model, there was rare research on landslide dam flood discharge and barely any models to simulate the progress of landslide flood discharge. Therefore, this study aims to: 1) construct the landslide dam flood discharge model by coupling DB-IWHR model and the two-dimensional hydrodynamic model; 2) simulate the process of Baige landslide dam flood discharge and verify the applicability of the coupled model; 3) multiple scenarios analysis on simulating landslide dam flood discharge by setting different spillway width and depth.

2 Materials

2.1 Study area

This study took Jinsha River, located at the upper reaches of the Yangtze River in China, as study area. The river starts from Yushu County of Qinghai Province and ends at Yibin of Sichuan Province. Its main stream is 3482 km long, and both sides of the Jinsha River are very steep. It is also a high incidence area of geological disasters. Topography of this area is very suitable to form landslide dams, and two landslide dam incidents occurred in this area. Zone A (Fig. 1) shows the location of the landslide dam, zone B (Fig. 1) represents main residential area.

2.2 Disaster progress

The first landslide occurred at the junction of Jiangda County of Tibet Autonomous Region and Baiyu County of Sichuan Province. It subsequently blocked trunk stream of the Jinsha River and formed the landslide lake at 22:06, October 10, 2018. The landslide lake began to overflow at 7:02, October 12th. There was a trapezoidal trough to discharge flood on the right slide of landslide dam with 160 m top width, 70 m bottom width and 55 m depth. After 160 min, the possibility of dam-break was excluded. However, Baige landslide dam, generated from the second landslide, also occurred at the same location, and formed landslide dam at 17:40, November 3, 2018. To eliminate disaster, an artificial discharge tank dug began to discharge flood at 10:50 a.m., November 12, 2018. Until 8:00 a.m. on November 15, 2018, the water level maintained stable and the disaster was obviated.

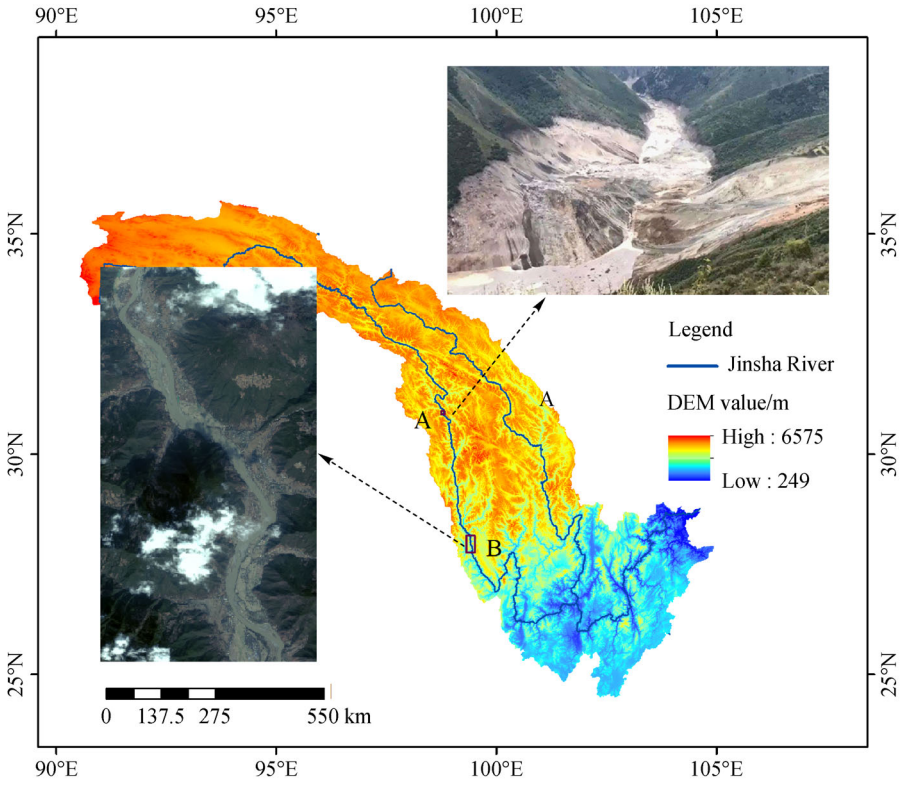

Fig. 1 The location of the study area. A: the location of Baige landslide dam. B: the location of residential area.

2.3 Data sources

Disaster site data from related literature (Chen et al., 2019; Hou et al., 2019) and reports (available at government website) was considered as parameters input for the coupled model. The parameters included geographical parameters, hydraulic parameters and geotechnical parameters (Wang et al., 2016), with the detailed information of these parameters as shown in Table 1.

DEM data was from SRTM, provided by Geospatial Data Cloud site, Computer Network Information Center, Chinese Academy of Sciences (available at Geospatial Data Cloud website). We used the measured river section by interpolation to form Jinsha River bed terrain, and this

Table 1 Main Parameters input for the coupled model

	Name	Symbol	Values
Geographical parameters	W~H curve coefficient	p_1, p_2, p_3	0.16, –1.51, 80.94
	Evaluations of reservoir water level, beginning/m	H_0	2956.17
	Inflow flow/($m^3 \cdot s^{-1}$)	Q_{in}	1500
	Evaluations of dead water/m	H_r	2903.94
	Evaluations of landslide dam/m	H_l	2963.5
Hydraulic parameters	Broad-crest Weir coefficient	m_q, m_b, m	0.36, 0.90, 0.80
	Initiated flow rate/($m \cdot s^{-1}$)	V_C(m/s)	4
	Erosion coefficient	a, b	1.1, 0.0004
	Manning coefficient	n	0.04
	Courant number	CFL	0.5
Geotechnical parameters	Dam material parameters	γ, c, φ,	16 kN/m^3, 30 KPa, 25°
	Burst model parameters	m_1, m_2	0.2700, 0.0245
	Evaluations of channel bed/m	z_0	2952
	Channel width, beginning/m	B_0	22

work have been done by Professor Hou from Xi'an University of Technology (Hou et al., 2019).

Satellite image with 2m-resolution used in the paper was GaoFen-1 (GF-1) image in the progress of the rational polygon coefficient (RPC) correction and fusion between multispectral data (8 m spatial resolution) and panchromatic data (2 m spatial resolution). GF-1 satellite main parameters are shown in Table 2 (Wang et al., 2018b).

Table 2 Parameters of GF-1 satellite (Wang et al., 2018b)

Parameter		Value
Resolution	Multispectral	8 m
	Panchromatic	2 m
	Wide field viewer	16 m
Image width	Multispectral and panchromatic	60 km
	Wide field viewer	800 km
Revisit cycle		4 days

3 Methodology

3.1 The coupled model construction

The coupled model combined DB-IWHR model and two-dimensional hydrodynamic model to simulate landslide dam flood discharge. Core process of simulating landslide dam flood discharge mainly included two steps: 1) simulate landslide dam flood discharge flow duration curve in spillway by the DB-IWHR model; 2) simulate landslide dam flood discharge inundation by the two-dimensional hydrodynamic model (2D model). Flow chart of the coupled model is shown in Fig. 2. First, Geographical parameters, hydraulic parameters and geotechnical parameters were input for the DB-IWHR model, the output was flow duration curve in spillway. Then, the flow duration curve, satellite imagery and DEM data were input for the two-dimensional hydrodynamic model to simulate the extent of flood area. The coupled model runs at a timestep of 2 min and does not need a spin-up period.

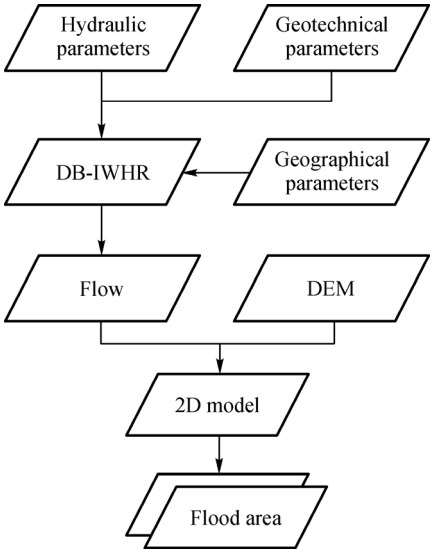

Fig. 2 Flow chart of the coupled model.

3.1.1 Flow simulation

Once the landslide dam formed, the dam parameters and inflow were always certain. The way of landslide dam flood discharge was digging the spillway, and DB-IWHR model provided the way to establish connection between the width and depth above water of spillway and the discharge curve during the flood discharge. DB-IWHR model was developed based on physical mechanism. The key simulated processes of DB-IWHR model contained three core portions:

1) Outflow though spillway was adopted the hydraulics of a broad-crested weir (Chen et al., 2019):

$$Q = CB(H - z)^{\frac{3}{2}}, \tag{1}$$

where Q is outflow in spillway, unit in m^3/s; C is discharge coefficient, unit in $m^{1/2}/s$; B is width of spillway, unit in m; H is evaluations of reservoir water level, beginning, unit in m; z is evaluations of spillway, unit in m.

2) A hyperbolic model was proposed in DB-IWHR model, which takes the following form (Chen et al., 2015b):

$$\dot{z} = \Phi(\tau)^{\frac{3}{2}} = \frac{U}{a + bU}, \tag{2}$$

$$U = k(\tau - \tau_c), \tag{3}$$

where $\dot{z}$ is erosion rate, unit in 10^{-3}mm/s; U is shear stress with reference to its critical component; k is unit conversion factor.

3) Breach lateral enlargement procedure of DB-IWHR model adopted circular slip surfaces method which has been widely accepted in geotechnical field. The process was repeated among various possible slip surfaces for calculating the factor of safety until an important one corresponding to the minimum of safety factor was found and was simplified in practice (Chen et al., 2015b).

12 parameters, such as W~H curve coefficient, evaluations of reservoir water level, inflow flow, evaluations of dead water, evaluations of landslide dam, broad-crest weir coefficient, initiated flow rate, erosion coefficient, dam material parameters, burst model parameters, evaluations of spillway bed and spillway width, were used as input parameters for DB-IWHR model (Table 1). DB-IWHR model was relatively less sensitive to the input parameters based on this hyperbolic model. Meanwhile, the model adopted a new solution technique that integrated the flow process based on velocity increment and solved the

governing equation directly without iterative arithmetic (Wang et al., 2016).

3.1.2 Flood discharge simulation

Two-dimensional hydrodynamic model was adopted in the research to simulat the landslide dam flood discharge routing, which was essentially the shallow water equations based on numerical solution. It was popular to simulate most of two-dimensional free surface flow (Li et al., 2019; Yin et al., 2019). Two-dimensional hydrodynamic model took Saint-Venant equations as governing equations as follows (Li et al., 2019):

The continuous equation:

$$\frac{\partial h}{\partial t}+\frac{\partial U}{\partial x}+\frac{\partial V}{\partial y}=Q. \tag{4}$$

The momentum equation:

$$\frac{\partial U}{\partial t}+\frac{\partial (uU)}{\partial x}+\frac{\partial (vV)}{\partial y}+gh\frac{\partial H}{\partial x}+g\frac{n^2u\sqrt{u^2+v^2}}{h^{1/3}}=0, \tag{5}$$

$$\frac{\partial V}{\partial t}+\frac{\partial (uV)}{\partial x}+\frac{\partial (vV)}{\partial y}+gh\frac{\partial H}{\partial x}+g\frac{n^2v\sqrt{u^2+v^2}}{h^{1/3}}=0, \tag{6}$$

where t is time, unit in s; U and V are the speed in the X and Y direction respectively, unit in m^3/s; H is water level, unit in m; h is water depth, unit in m; n is roughness coefficient.

The upper boundary was the flow duration curve in spillway from the DB-IWHR model. Meanwhile, we considered the special level as a lower boundary. The paper adopted 0.04 as the roughness coefficient (Chen et al., 2019), and simulated a total of 8 h landslide dam flood discharge progress.

3.2 Flood maximum extent mapping

Mapping of flood maximum extent was interpreted from the GF-1 Satellite imagery obtained on November 13, 2018. There were three rules to determine flood maximum extent (Renschler and Wang, 2017): 1) physical evidence by river deposits arranging in a linear pattern and mostly paralleling to the flow direction; 2) interpretation of satellite imagery through comparing the color and brightness from no-flooded zone with previously flooded areas; 3) marker interpretation by looking for traces of flood damage, such as housing damage, impervious surface sediment deposition, plants dump and so on. Hence, the trace of the flood was very evident on the GF-1 satellite image based on the second rule.

3.3 Accuracy evaluation

To ensure the accuracy of simulated results by the coupled model, we used remote sensing image (GF-1 image) after the flood discharge to compare the inundated area between actual inundated area and the simulated inundated area. Fit statistic (F) was suitable to evaluate the degree of match between actual inundated area and the simulated inundated area, and its value arranged from 1 to 0, the less it was, the more difference between actual inundated area and the simulated inundated area (Renschler and Wang, 2017). It was computed as follows:

$$F=\frac{n_0}{n_r+n_v-n_0}, \tag{7}$$

where n_v and n_r are number of pixels in simulated inundated area and observed inundated area. n_0 is the overlap of n_v and n_r.

3.4 Multiple scenarios analysis

From the perspective of disaster relief and mitigation, sensitivity of depth and width for the coupled model is important to support disaster relief and mitigation. Therefore, based on the actual spillway parameters in the Baige landslide dam flood charge, model sensitivity to spillway parameters are detected by regularly varying width and depth of spillway respectively (Table 3).

To test spatiotemporal change of flood charge inundation, Root Mean Square Deviation (*RMSD*) and F are adopted to qualify the change of inundated area and water depth between multiple scenario simulation and scenario Baige. The *RMSD* was widely used to quantify the water depth deviation between real scenario simulation and virtual scenario simulation at the same unit, the more difference between the two scenarios, the larger it was. The formula was computed as follows (Willmott, 1981):

$$RMSD=\sqrt{\frac{\sum_{i=1}^{n}(v_i-r_i)^2}{n}}, \tag{8}$$

where n is the number of wet pixels to assess; v_i and r_i are water depths at location i pixel in virtual scenario inundated area and real scenario inundated area.

4 Results and discussion

4.1 Flood discharge simulation

Figure 3 shows the Baige landslide dam flood discharge flow duration curve in spillway. After 1.5 h of the flood discharge beginning, the flow value was very small and increased very slowly. From 1.5 h to approximate 4 h, one remarkable feature was that the flow value increased very quickly, approximately after 4 h later, the flow reached the

Table 3 Multiple scenarios simulated by coupled model

Scenario name	Elevation of spillway bed/m	Elevation of water level/m	Spillway width/m	Spillway depth/m
1	2952	2956.17	2	11.5
2	2952	2956.17	12	11.5
3	2952	2956.17	32	11.5
4	2952	2956.17	42	11.5
5	2948	2956.17	22	15.5
6	2950	2956.17	22	13.5
7	2954	2956.17	22	9.5
8	2956	2956.17	22	7.5
Baige	2952	2956.17	22	11.5

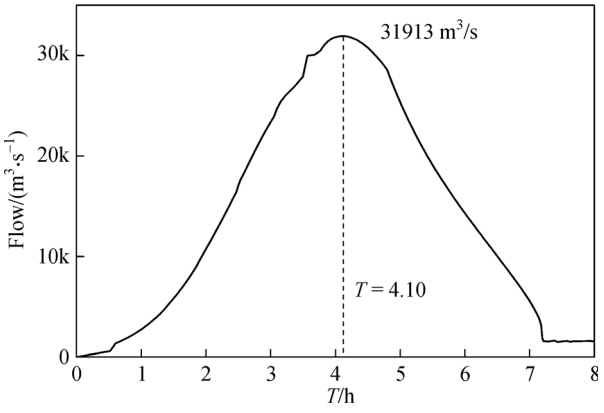

Fig. 3 Baige landslide dam flood discharge flow duration curve of in spillway.

maximum value, exceeding 31000 m^3/s, which was about the same as the news report (available at Sichuan Government website). The flow value then began to fall and was stable after 7 h. Other feature was the smoothness of the flow duration curve, there were more than one inflection points on the flow duration curve until 4 h, the flow duration curve was relatively smooth after that. This phenomenon revealed stronger erosion of spillway at the beginning progress of flood discharge.

The progress of landslide dam flood discharge simulated by the coupled model is shown in Fig. 4 beginning at 10:50 a.m. on November 12, 2018. The results showed that the flood quickly flowed along the riverbed. The flood arrived at Renda after 2 h, and arrived at Kamai after 4 h, and 6 hours later, it arrived at Dengba. It finally arrived at Huotang within the simulated progress period. For the flow traveling distance, the stream flow distance exceeded 2000 m and the maximum water depth approached 6 m by 11:50 (Fig. 4(a)), meanwhile, the stream flow distance per hour was 2167 m, 6147 m, 7961 m, 9325 m, 11700 m, 10795 m, 12905 m respectively (Fig. 4). The results demonstrated that the stream flow distance per hour had large differences and increased in 4 h but reduced 4 h after. The reason was that the larger flow value was, the quicker flow was. We concluded that flow distance was related to both flow and the topographic conditions, and the change of maximum water depth was also subject to similar tendency. Figure 4 shows that the max water depth was increasing in the first four hours and appeared at between 4 h and 5 h. After that, it sustained steadily. Combined with Fig. 3 analysis, that peak flow appeared during this period was concluded.

Figure 5 clearly presents the flood inundated area and maximum water depth after 8 h of the landslide dam flood discharge. The inundated area distributed along the river channel and flood plain on both sides. 10 residential areas were threatened in the period of flood discharge, such as Keri was partially submersed, which was consistent with the news report (available at iFeng website). Region A and B were randomly selected which were superimposed on Google Earth image to demonstrate flood discharge in details. To qualitatively verify the accuracy of simulated result, the simulated flood discharge evolution from the coupled model was roughly according with actual river flood evolution characteristics and there was good match on inundated area between the simulation and observation (i.e., GF-1 image) as shown in Fig. 5. This coupled model which was suitable to simulate the landslide dam flood discharge was concluded.

4.2 Maximum flood extent map

Figure 6 shows the location of verified area selected randomly which was illustrated with black rectangle. Figure 6(a) was obtained from GF-1 false color image with 2 m spatial resolution on November 13, 2018. Inundated area contained river channel and both sides inundated area. Color and brightness of landslide dam inundated area were different from no-inundated area, the red box extent was maximum inundated area caused landslide dam flood discharge. Figure 6(b) shows the superposition of inundated area and simulated inundated area. To quantitatively verify the accuracy of simulated result, the F value between inundated area and simulated inundated area was 80.05%, and it showed the high consistent of inundated

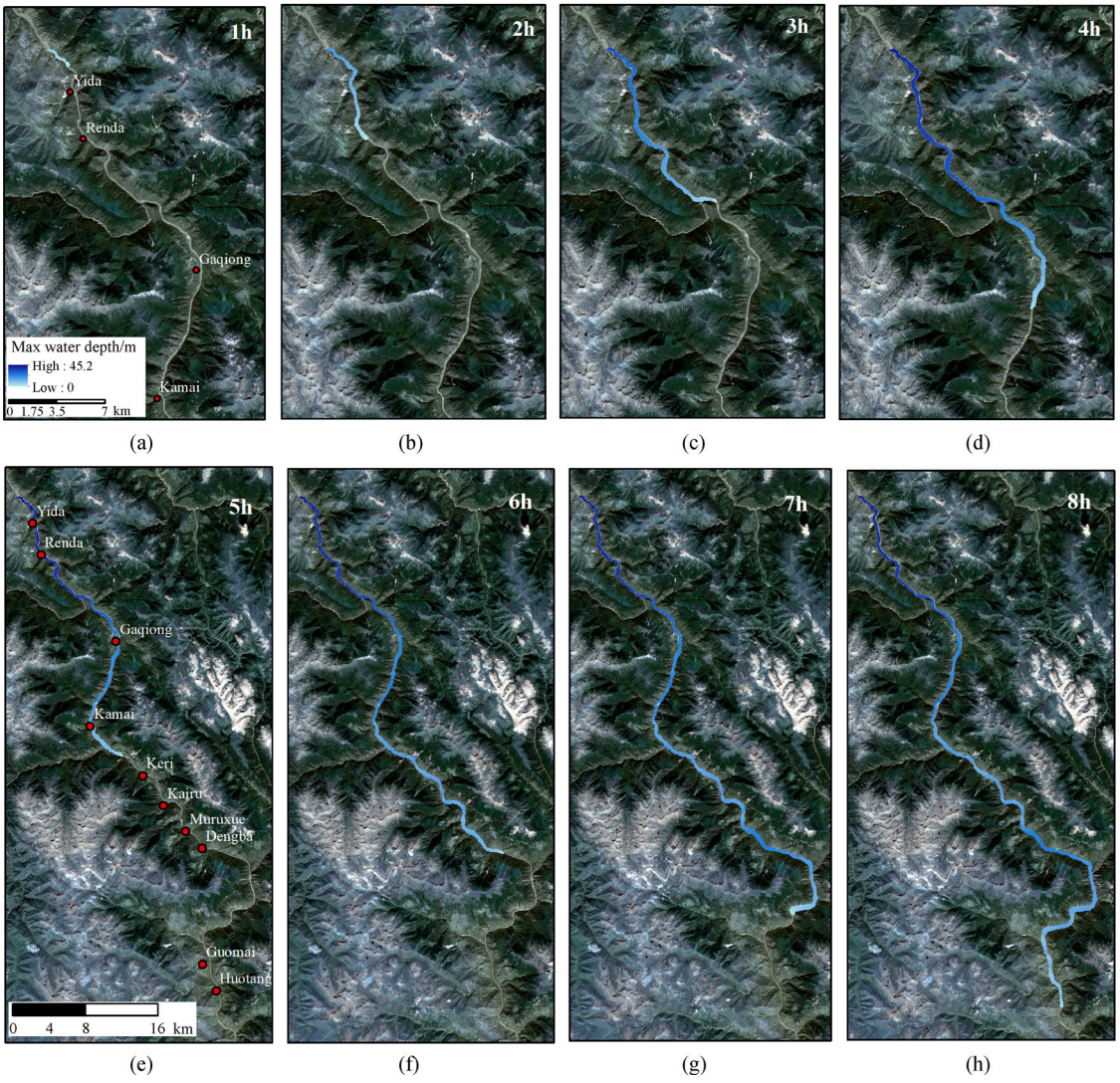

Fig. 4 Process of simulated landslide dam flood discharge inundation.

area and simulated inundated area. The result indicated that the coupled model was suitable to simulate landslide dam flood discharge.

The coupled model mainly highlighted the model as flow duration curve in spillway and the complex unsteady flow calculated. As landslide dam flood discharge extent prediction model for emergency rescue, it must have higher accuracy and rapid response mechanism to ensure effectiveness of the relief efforts. This coupled model was coupled by DB-IWHR model and two-dimensional hydrodynamic model. The input parameters for the coupled model were simpler, and the coupled model ran steadily and cost less time. It perfectly presented the whole progress of landslide dam flood discharge and obtained higher accuracy results by verification with high resolution remote sensing image monitoring results.

The simulated result completely repeated the progress of Baige landslide dam flood discharge in this paper. The relative parameters were used as inputs and landslide dam flood inundated area was as output from the coupled model. Previous research paid attention to the urban flood and focused on analysis of the importance of topography, mesh resolution, resistance parameter, DEM sources et al. on the hydrodynamic simulation (Horritt and Bates, 2002; Begnudelli and Sanders, 2007; Schubert et al., 2008; Gallegos et al, 2009). In the aspect of the landslide dam disaster mitigation and relief, spillway width and depth directly decided successful rate of disaster reduction. It was very important to determine the effect of change of spillway widths and depths to the flood discharge flow duration curve and arrival time of peak flow in spillway, so as to analyze the effect of landslide dam flood inundated area and water depth at river cross-section. Therefore, Section 4.3 presented eight scenarios by setting different spillway depth and spillway width for the coupled model in Table 3. Multiple scenarios simulation experiments

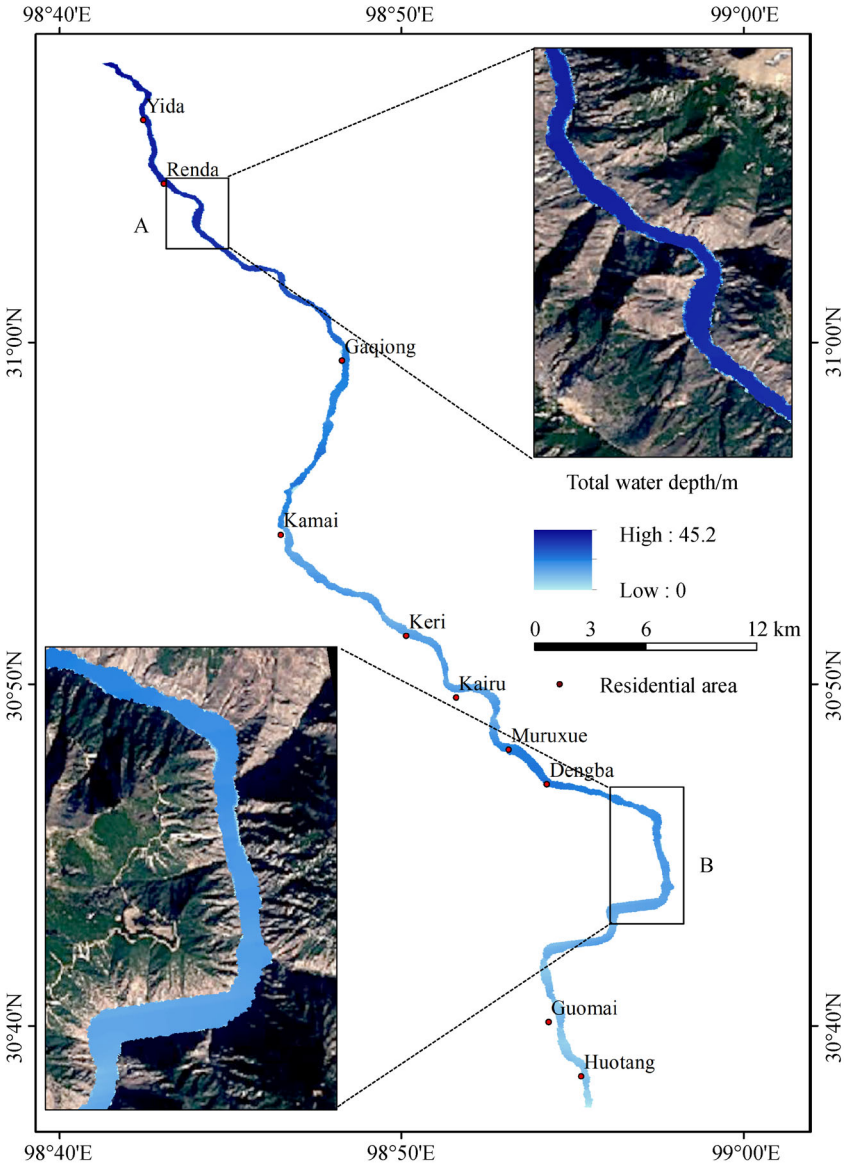

Fig. 5 Baige landslide dam flood discharge inundation mapping.

attempted to determine the effect of setting different spillway depth and spillway width regularly on flow duration curve in spillway, arrival time of peak flow in spillway, inundated area and water depth at river cross-section.

4.3 Multiple scenarios simulation

This section simulated different scenarios by regularly setting spillway width and depth as shown in Table 3. Scenarios 1–4 expressed that spillway width increased at an interval of 10 m with fixed spillway depth. On the contrary, scenarios 5–8 displayed that spillway depth decreased at an interval of 2 m with fixed spillway width.

Figure 7 shows the landslide dam flood discharge flow duration curve of scenarios 1–4 in spillway. First of all, the result distinctly showed both initial flow occurrence time and value increased with the increasing of spillway width. The rate of the increasing flow gradually became greater with the increasing of spillway width in the initial period of flood discharge. It was noted that scenario 1 had no initial flow as shows in Fig. 7, however, it presented the initial flow was very small instead of no flow. To sum up, this phenomenon depicted less erosion with larger width, leading to the greater flow at the initial stage of landslide dam flood discharge. Then, both the peak flow and its arrival time presented slightly tendency of decrease with the increasing of spillway width. At last, the smoothness of flood discharge flow duration curves was basically similar, and there were no obvious difference flood discharge flow

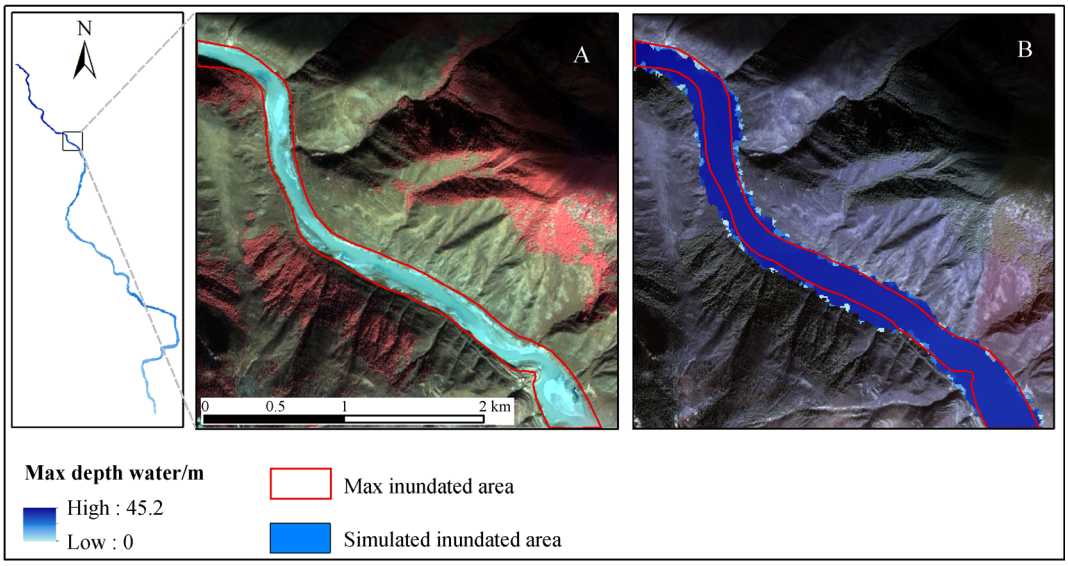

Fig. 6 Max landslide dam flood discharge mapping. A: maximum inundated area map from false color GF-1 image. B: simulated inundated area.

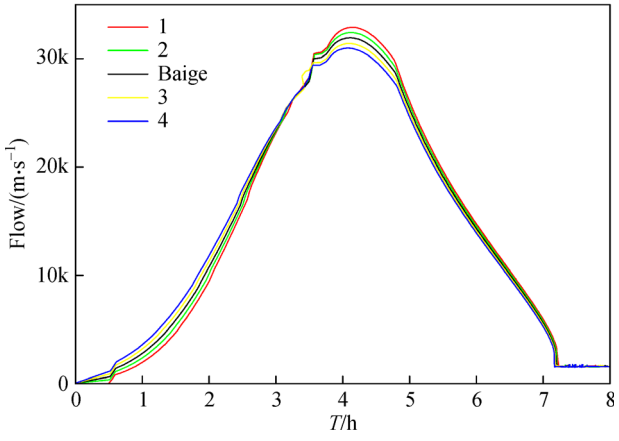

Fig. 7 Landslide dam flood discharge flow duration curves of scenarios 1–4 in spillway.

duration curves in these scenarios. In addition, it meant erosion on both sides and bottom of spillway by flood flow was more stable. In conclusion, spillway width was not sensitive to peak flow and its arrival time in spillway.

The corresponding inundated area of scenarios 1–4 are in Fig. 8. In term of qualitative analysis, there was slight difference between scenario Baige simulation result (Fig. 5) and scenarios 1–4 results (Fig. 8). The landslide dam flood flowed through Huotang in all above scenarios and flood routing distance became shorter when spillway width increased from 2 m to 42 m at 10 m interval. For the river was not wide, water depth was similar at same river cross-section. Figure 9 shows the relationship between flood routing distance and water depth at river cross-section in scenarios 1–4. The result of quantitative analysis showed that water depth at every river cross-section decreased with the increasing of spillway width at 10m interval (Fig. 9). In general speaking, the deeper water depth at river cross-section, the larger the inundation area in same region (Zhang et al., 2015). When spillway width decreased from 22 m to 2 m at 10m interval, water depth at every river cross-section averagely increased by 1.52 m and 1.62 m and inundated area approximately increased by 2.85% and 2.67% in scenarios 1–2. On the contrary, when spillway width increased from 22 m to 42 m at 10 m interval, water depth at every river cross-section averagely decreased by 1.84 m and 1.64 m and inundated area approximately decreased by 1.48% and 2.63% in scenarios 3–4 respectively (Table 4).

Scenarios 1–4 results showed that spillway width was not sensitive to water depth at river cross-section and the inundated area, and water depth at river cross-section and the inundated area decreased with the increasing of spillway width. Even if the variation of spillway width was at 10 m interval, the average variation of water depth was less than 1.82 m and the variation of inundated area was less than 2.85%. Water depth at river cross-section reached the maximum in scenario 1, and the minimum in scenario 4, meanwhile inundated area reached the maximum in scenario 1 and the minimum in scenario 4.

Similarly, Fig. 10 shows landslide dam flood discharge flow duration curves of scenarios 5–8 in spillway. First of all, the rate of the increasing flow was increased with the increasing of spillway depth at 2 m interval, and flow duration curves of scenarios 5–6 and scenario Baige were smoother than scenarios 7–8 at beginning of landslide dam flood discharge. Hereafter, arrival time of peak flow and peak flow increased with the decreasing of spillway depth at 2 m interval in scenarios 5–6, but the rule did not obviously present in scenarios 7–8. Lastly, the flow

Fig. 8 Landslide dam flood discharge inundation mapping of scenarios 1–4.

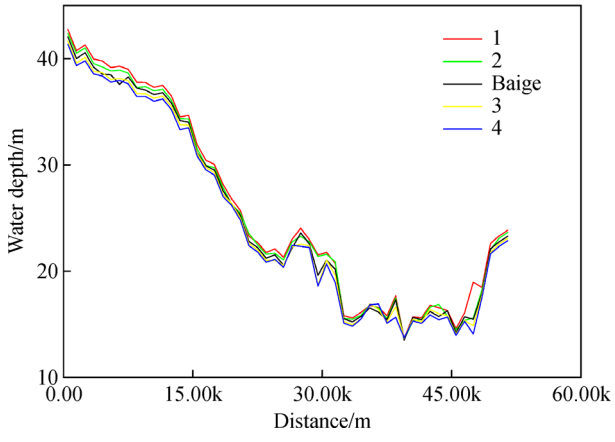

Fig. 9 The relationship between flood routing distance and water depth at river cross-section in scenarios 1–4.

duration curves of scenarios 5–8, especially scenarios 7–8, were not smooth. This phenomenon might be caused by stronger erosion of the flow on spillway bottom and both sides in scenarios 7–8. Meanwhile, the stronger erosion also caused that arrival time of peak flow were obviously behind scenarios 5–6, it also caused obvious change of flow in a short period. Spillway depth was more sensitive to arrival time of peak flow and peak flow in spillway than spillway width.

Figure 11 shows the landslide dam flood inundated area of scenarios 5–8. The landslide dam flood flowed through Huotang in scenarios 5–7, however, scenario 8 flood did not flow through Guomai by qualitative analysis. Flood routing distance gained maximum value in scenario 7, and it obviously shortened in else scenario. In aspect of quantitative analysis, Fig. 12 shows water depth at every river cross-section reached the maximum in scenario 7 and the minimum in scenario 5. On the one hand, when spillway depth decreased from 11.5 m to 7.5 m at 2 m interval, water depth at every river cross-section averagely decreased by 2.36 m and 2.10 m and the inundated area approximately decreased by 2.85% and 5.70% in scenario 5 and in scenario 6 respectively. On the other hand, when spillway depth increased from 11.5 m to 15.5 m at 2 m interval, water depth at every river cross-section averagely increased by 1.77 m in scenario 7 and averagely decreased

Table 4 *F* and *RMSD* between the simulated results of scenarios 1–4 and scenario Baige

Scenario	Spillway width/m	Spillway depth/m	*F*/%	*RMSD*/m
1	2	11.5	97.15	1.62
2	12	11.5	97.33	1.52
Baige	22	11.5	100	0
3	32	11.5	98.52	1.82
4	42	11.5	97.37	1.64

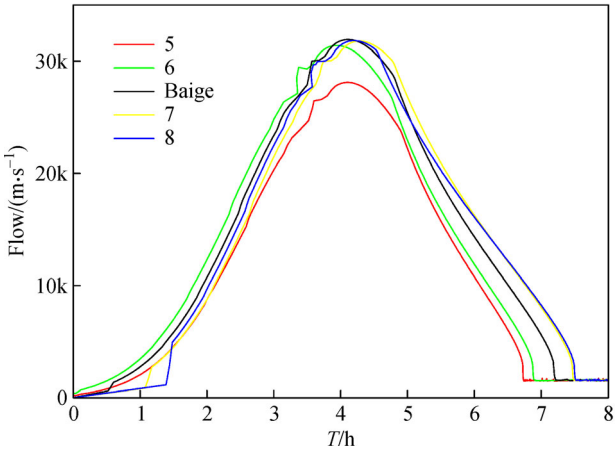

Fig. 10 The flood discharge flow duration curves of scenarios 5–8 in spillway.

by 2.18 m in scenario 8, meanwhile the inundated area approximately increased by 6.54% in scenario 7 and decreased by 12.37% in scenario 8 (Table 5).

Scenarios 5–8 results indicated that spillway depth was more sensitive to water depth at river cross-section and the inundated area than spillway width, and water depth at river cross-section and the inundated area increased then started to drop, as spillway depth kept decreasing. When the variation of spillway depth was at only 2 m interval, the average variation of water depth basically exceeded 2 m and the variation of inundated area was more than 2.85%. Water depth at river cross-section reached the maximum in scenario 7 and the minimum in scenario 5, meanwhile inundated area reached the maximum in scenario 7 and the minimum in scenario 5.

5 Conclusions

The main outcomes are as follow:

1) From the perspective of landslide dam disaster relief, this study integrated DB-IWHR model and two-dimensional hydrodynamic model to build the coupled model with the advantages of simple operation and less time consuming for simulating the process of landslide dam flood discharge.

2) The research also simulated the progress of the Baige landslide dam flood discharge using the coupled model, and, verified by remote sensing image monitoring result,

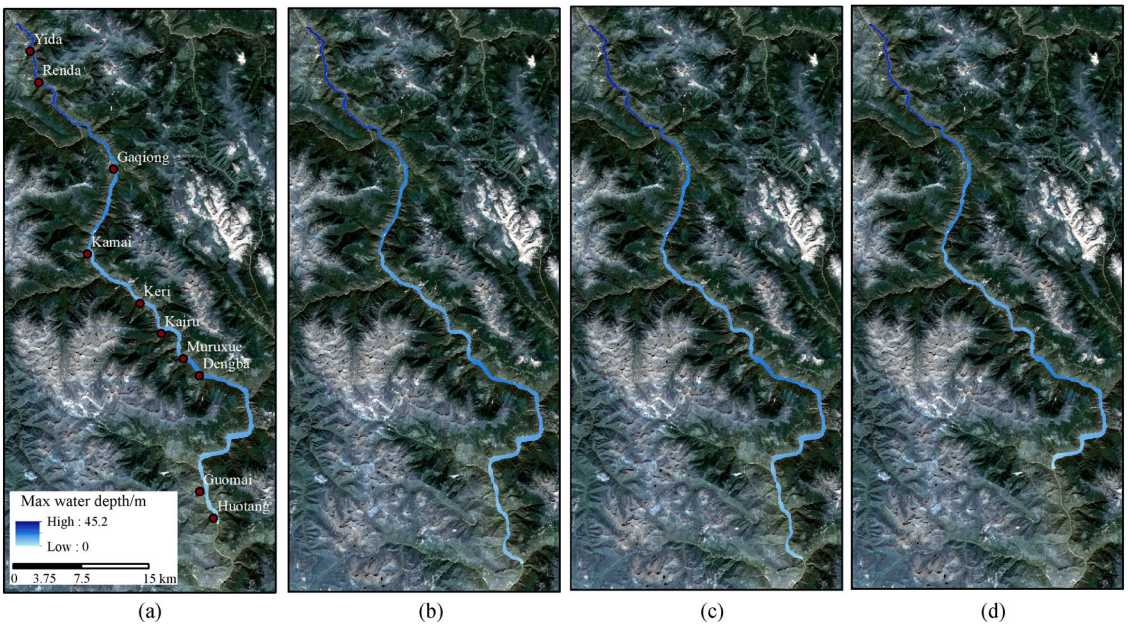

Fig. 11 Landslide dam flood discharge inundation mapping of scenarios 5–8.

Table 5 *F* and *RMSD* between the simulated results of scenarios 5–8 and scenario Baige

Scenario	Spillway width/m	Spillway depth/m	*F*/%	*RMSD*/m
5	22	15.5	97.15	2.36
6	22	13.5	94.30	2.10
Baige	22	11.5	100	0
7	22	9.5	93.46	1.77
8	22	7.5	87.63	2.18

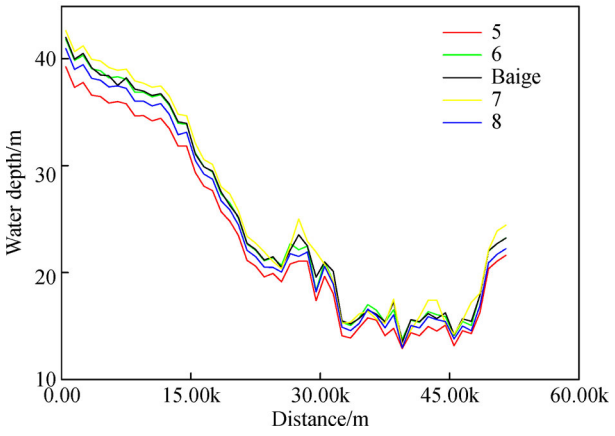

Fig. 12 The relationship between flood routing distance and water depth at river cross-section in scenarios 5–8.

the results of the simulation obtained high accuracy. Landslide dam flood distance is relative to the flow and the topographic conditions by analyzing process of Baige landslide dam flood discharge.

3) Spillway width presents low sensibility to arrive time of peak flow and peak flow in spillway, and also water depth at river cross-section and the inundated area by analyzing scenarios 1–4. Water depth at river cross-section and the inundated area decrease with the increase of spillway width. Even if spillway width varies at 10 m interval, the average variation of water depth is less than 1.82 m and the variation of inundated area is less than 2.85%.

4) Spillway depth is sensitive to arrive time of peak flow and peak flow in spillway, and also water depth at river cross-section and the inundated area by analyzing scenarios 5–8. Water depth at river cross-section and the inundated area increase then start to drop, as spillway depth keeps decreasing. When spillway depth varies at only 2 m interval, the average variation of water depth at river cross-section basically exceeds 2 m and the variation of inundated area is more than 2.85%.

Acknowledgements This work was supported by the National Key Research and Development Program of China (Grant Nos: 2017YFB0504100 and 2016YFC0803000).

References

Ahmad I, Verma M K (2018). Application of analytic hierarchy process in water resources planning: a GIS based approach in the identification of suitable site for water storage. Water Resour Manage, 32(15): 5093–5114

Basabe P T (2013). Encyclopedia of natural hazards. Encyclopedia of Earth Sciences, 28(2): 36

Begnudelli L, Sanders B F (2007). Simulation of the St. Francis dam-break flood. J Eng Mech, 133(11):1153–1161

Brown R J, Rogers D C (1981). BRDAM Users Manual. Denver: U.S. Dept. of the Interior, Water and Power Resources Service

Brunner G W (2016). HEC-RES River Analysis System-User's Manual Version 5.0. US Army Corps of Engineers. Institute for Water Resources, Hydrologic Engineering Center (HEC). 962

Cenderelli D A (2000). Floods from natural and artificial dam failures. In: Wohl EE., ed. Inland Flood Hazards. Cambridge: Cambridge University Press

Chai H J, Liu H C, Zhang Z Y (1995). The catalog of Chinese landslide dam events. J Geol Hazards Env Preserv, 6(1): 1–9 (in Chinese)

Chang D S, Zhang L M (2010). Simulation of the erosion process of landslide dams due to overtopping considering variations in soil erodibility along depth. Nat Hazards Earth Syst Sci, 10(4): 933–946

Chen R F, Chang K J, Angelier J, Chan Y C, Deffontaines B, Lee C T, Lin M L (2006). Topographical changes revealed by high-resolution airborne LiDAR data: the 1999 Tsaoling landslide induced by the Chi-Chi earthquake. Eng Geol, 88(3): 160–172

Chen X, Cui P, You Y, Chen J, Li D (2015a). Engineering measures for debris flow hazard mitigation in the Wenchuan earthquake area. Engineering Geological, 194(SI): 73–85

Chen Z, Ma L, Yu S, Chen S, Zhou X, Sun P, Li X (2015b). Back analysis of the draining process of the Tangjiashan Barrier Lake. J Hydraul Eng, 141(4): 05014011

Chen Z Y, Zhang Q, Hou J M, Wang L, Ma L P (2019). Back analysis on dam-breach flood of "10.10" Baige barrier lake on Jinsha River. Yangtze River, 50(5): 1–4 (in Chinese)

Cook A C (2008). Comparison of one-dimensional HEC-RAS with two-dimensional FESWMS Model in flood inundation mapping. Dissertation for Master's Degree. West Lafayette: Purdue University

Costa J E, Schuster R L (1988). The formation and failure of natural dams. Geol Soc Am Bull, 100(7): 1054–1068

Costa J E, Schuster R L (1991). Documented historical landslide dams from around the world. US Geol Surv Open-File Rep: 91–239

Costa J E (1985). Floods from dam failures. U.S. Geological Survey Open-File Rep. No. 85–560, U.S. Geological Survey, Denver

Cristofano E A (1965). Method of computing erosion rate of failure of earth dams. Denver: U.S. Bureau of Reclamation

Dai F C, Lee C F, Deng J H, Tham L G (2005). The 1786 earthquake-triggered landslide dam and subsequent dam-break flood on the Dadu River, southwestern China. Geomorphology, 65(3–4): 205–221

Dong J J, Tung Y H, Chen C C, Liao J J, Pan Y W (2009). Discriminant analysis of the geomorphic characteristics and stability of landslide dams. Geomorphology, 110(3–4): 162–171

Evans S G, Delaney K B, Hermanns R L, Strom A, Scarascia-Mugnozza G (2011). The formation and behavior of natural and artificial rockslide dams: implications for engineering performance and hazard management. In: Evans S G, Hermanns R L, Strom A L, Scarascia Mugnozza G, eds. Natural and artificial rockslide dams. Lecture Series in Earth Sciences. Berlin: Springer, 1–76

Ermini L, Casagli N (2003). Prediction of the behavior of landslide dams using a geomorphological dimensionless index. Earth Surf Process Landf, 28(1): 31–47

Evans S G (1986). The maximum discharge of outburst floods caused by the breaching of man-made and natural dams. Can Geotech J, 23(3): 385–387

Fan X M, Cees J, Westen V, Korup O, Gorum T, Xu Q, Dai F C, Huang R Q, Wang G H (2012). Transient water and sediment storage of the decaying landslide dams induced by the 2008 Wenchuan earthquake, China. Geomorphology, 171–172: 58–68

Fread D L (1984). DAMBRK: The NWS dam break flood forecasting model. National Oceanic and Atmospheric Administration, National Weather Service, Silver Spring

Fread D L (1988). BREACH: an erosion model for earthen dam failure. National Oceanic and Atmospheric Administration, National Weather Service, Silver Spring

Gallegos H A, Schubert J E, Sanders B F (2009). Two-dimensional, high-resolution modeling of urban dan-break flooding: a case study of Baldwin Hills, California. Adv Water Resour, 32(8): 1323–1335

Gorum T, Fan X M, Westen C J, Huang R, Xu Q, Tang C, Wang G (2011). Distribution pattern of earthquake-induced landslides triggered by the 12 May 2008 Wenchuan earthquake. Geomorphology, 133(3–4): 152–167

Hermanns R L, Folguera A, Penna I, Fauqué L, Niedermann S (2011). Landslide dams in the central Andes of Argentina (Northern Patagonia and the Argentine Northwest). In: Evans S G, Hermanns R L, Strom A L, Scarascia Mugnozza G, eds. Natural and Artificial Rockslide Dams. Lecture Series in Earth Sciences. Berlin: Springer, 147–176

Horritt M S, Bates P D (2002). Evaluation of 1D and 2D numerical models for predicting river flood inundation. J Hydrol (Amst), 268 (1–4): 87–99

Hou J M, Ma L P, Chen Z Y, QI W C, Wang L (2019). High-performance numerical simulation for dam-break flood propagation of Baige barrier lake in Jinsha River. Yangtze River, 50(4): 65–70 (in Chinese)

Keefer D K (1984). Landslides caused by earthquakes. Geol Soc Am Bull, 95(4): 406–421

Knebl M R, Yang Z L, Hutchison K, Maidment D R (2005). Regional scale flood modeling using NEXRAD rainfall, GIS, and HEC-HMS/RAS: a case study for the San Antonio River Basin Summer 2002 storm event. J Environ Manage, 75(4): 325–336

Korup O (2002). Recent research on landslide dams—a literature review with special attention to New Zealand. Prog Phys Geogr, 26(2): 206–235

Korup O (2004). Geomorphometric characteristics of New Zealand landslide dams. Eng Geol, 73(1–2): 13–35

Korup O, Tweed F (2007). Ice, moraine, and landslide dams in mountainous terrain. Quat Sci Rev, 26(25): 3406–3422

Li W J, Lin K R, Zhao T G, Lan T, Chen X H, Du H W, Chen H Y (2019). Risk assessment and sensitivity analysis of flash floods in ungauged basins using coupled hydrologic and hydrodynamic models. J Hydrol (Amst), 572: 108–120

Mandrone G, Clerici A, Tellini C (2007). Evolution of a landslide creating a temporary lake: successful prediction. Quat Int, 171: 72–79

Morris M W, Galland J C (1988). CADAM: Dam Break Modeling Guideline & Best Practice. Munich: HR Wallingford Ltd.

O'Connor J E, Costa J E (2004). The world's largest floods, past and presented—their causes and magnitudes. Geol Surv Circ, 1254: 1–13

O'Connor J E, Beebee R A (2009). Floods from natural rock-material dams. Mega Flooding on Earth and Mars, 128–163

Pender G (2006). Briefing: introducing the flood risk management research consortium. Proc Inst Civ Eng Water Management, 159(1): 3–8

Peng M, Zhang L M (2012). Breaching parameters of landslide dams. Landslides, 9(1): 13–31

Renschler C S, Wang Z H (2017). Multi-source data fusion and modeling to assess and communicate complex flood dynamic to support decision-making for downstream areas of dams: the 2011 hurricane irene and Schoharie creek floods, NY. International Apply Earth Observation Geoinformation, 62: 157–173

Roberts S, Nielsen O, Gray D, Sexton J, Davies G (2015). ANUGA User Manual. Commonwealth of Australia and the Australian National University

Schubert J E, Sanders B F, Smith M J, Wright N G (2008). Unstructured mesh generation and landcover-based resistance for hydrodynamic modeling of urban flooding. Adv Water Resour, 31(12): 1603–1621

Schuster R L (1995). Landslide dams—a worldwide phenomenon. Landslides, 31(4): 38–49

Smith L C (1997). Satellite remote sensing of river inundation area, stage, and discharge: a review. Hydrol Processes, 11(10): 1427–1439

Singh V P, Scarlatos P D, Collins J G, Jourdan M R (1988). Breach erosion of earth-fill dams (BEED) model. Nat Hazards, 1(2): 161–180

Teng J, Jakeman A J, Vaze J, Croke B F W, Dutta D, Kim S (2017). Flood inundation modelling: a review of methods, recent advances and uncertainty analysis. Environ Model Softw, 90: 201–216

Viero D P, Peruzzo P, Carniello L, Defina A (2014). Integrated mathematical modeling of hydrological and hydrodynamic response to rainfall events in rural lowland catchments. Water Resour Res, 50 (7): 5941–5957

Walder J S, O'Connor J E (1997). Methods for predicting peak discharge of floods caused by failure of natural and constructed earthen dams. Water Resour Res, 33(10): 2337–2348

Wang F, Okeke A C U, Kogure T, Sakai T, Hayashi H (2018a). Assessing the internal structure of landslide dams subject to possible pipingerosion by means of microtremor chain array and self-potential surveys. Eng Geol, 234: 11–26

Wang G H, Huang R Q, Kamai T, Zhang F Y (2013). The internal structure of a rockslide dam induced by the 2008 Wenchuan (Mw7.9) earthquake, China. Eng Geol, 156: 28–36

Wang Z, Bowles D S (2006). Three-dimensional non cohesive earthen dam breach model. Part I: theory and methodology. Adv Water Resour, 29(10): 1528–1545

Wang L, Chen Z, Wang N, Sun P, Yu S, Li S, Du X (2016). Modeling lateral enlargement in dam breaches using slope stability analysis based on circular slip mode. Eng Geol, 209: 70–81

Wang S X, Yang B L, Zhou Y, Wang F T, Zhang R, Zhao Q (2018 b). Three-dimensional information extraction from GaoFen-1 satellite images for landslide monitoring. Geomorphology, 309: 77–85

Willmott C J (1981). On the validation of model. Phys Geogr, 2(2): 184–194

Wu W (2013). Simplified Physically Based model of earthen Embankment Breach. J Hydraul Eng, 139(8): 837–851

Xu Q, Fan X M, Huang R Q, Westen C (2009). Landslide dams triggered by the Wenchuan earthquake, Sichuan Province, southwest China.

Bull Eng Geol Environ, 68(3): 373–386

Xu Y, Zhang L M (2009). Breaching parameters for earth and rockfill dams. J Geotech Geoenviron, 135(12): 1957–1970

Yin J, Zhao Q, Yu D P, Lin N, Kubanek J, Ma G Y, Liu M, Pepe A (2019). Long-term flood-hazard modeling for coastal areas using InSAR measurements and a hydrodynamic model: the case study of Lingang New City, Shanghai. J Hydrol (Amst), 571: 593–604

Zhang H Q, Liu S, Hu C W, Xu W H (2015). Emergency response on flooding and subsiding process for Levee-breach at Tongfu Section of Heilongjiang River. Studies and Discussions, 25(1): 65–69 (in Chinese)

Zhang J Y, Li Y, Xuan G X, Wang X G, Li J (2009). Overtopping breaching of cohesive homogeneous earth dam with different cohesive strength. Sci China Ser E-Tech Sci, 52(10): 3024–3029